

## Effect of temperature on the cyclic stress components of Inconel 738LC superalloy

Martin Petrevec<sup>1, a</sup>, Miroslav Šmíd<sup>2, b</sup>, Karel Obrtlík<sup>1, c</sup>, Jaroslav Polák<sup>1, d</sup>

<sup>1</sup>Institute of Physics of Materials of Sciences of the Academy of the Czech Republic, Žitkova 22,  
616 62 Brno, Czech Republic

<sup>2</sup>Faculty of Mechanical Engineering, Brno University of Technology, Technická 2, 616 69 Brno,  
Czech Republic

<sup>a</sup>petrevec@ipm.cz, <sup>b</sup>smid@ipm.cz, <sup>c</sup>obrtlik@ipm.cz, <sup>d</sup>polak@ipm.cz

**Keywords:** Low cycle fatigue, Superalloy, high temperatures, Hysteresis loop, Effective and internal stresses.

**Abstract.** Multiple step tests in strain control have been performed on cylindrical specimens of cast polycrystalline Inconel 738LC superalloy at 23, 500 and 800 °C in laboratory atmosphere to study the effect of temperature on the internal and effective cyclic stress components. At these temperatures, the evolution of the effective and internal stress components and effective elastic modules were derived from the hysteresis loops which were analysed according to the statistical theory of hysteresis loop. Cyclic hardening/softening curves and shortened cyclic stress-strain curves were obtained at three temperatures. Cyclic hardening/softening behaviour depends both on temperature and strain amplitude. Low amplitude straining was characterized by saturation of the stress amplitude. In high amplitude straining a pronounced hardening was found at room temperature and at 500 °C. Saturated behaviour was found at temperature 800 °C. The shortened cyclic stress-strain curves can be fitted by power law at three temperatures. They are shifted to lower stresses with increasing temperature. Observation of the surface revealed cyclic strain localization into persistent slip bands at all three temperatures. Cyclic stress-strain response is compared at all temperatures and discussed in relation to changes of internal and effective stress components and microstructural parameters of the material.

### Introduction

Inconel 738LC (IN 738LC) is a precipitation strengthened nickel base superalloy with excellent high temperature strength and hot corrosion resistance. It is widely used for the production of blades and disks of gas turbine engines [1]. The critical turbine parts are subjected to repeated elastic-plastic straining as a result of heating and cooling during start-up and shut-down periods [2]. Therefore, low cycle fatigue is an important factor in the design of the components and cyclic stress-strain and fatigue life data in a wide temperature up to high temperatures are necessary for design of these equipment. The hardening/softening behaviour and cyclic stress-strain curve of Inconel 738LC has been studied at room temperature [3] and at temperature 900 °C [4,5]

More detailed study of the sources of the high cyclic stress in this superalloy was not performed. The shape of the hysteresis loop in cyclic straining can yield valuable information on the sources of the cyclic stress. The analysis of the loop shape allows the separation of the total cyclic stress into the effective and the internal stress components [6]. This method is based on the generalized statistical theory of the hysteresis loop and has also been used in the analysis of the cyclic plasticity in stainless steels [7,8]. It originates from the Masing approach to the cyclic plasticity of crystalline materials according to which the individual microvolumes of the crystal undergo equal strain but carry different stresses. According to the generalized statistical theory of the hysteresis loop [6], the stresses carried by individual microvolumes can be separated into the effective and the internal stress components. In each plasticized volume the effective stress is the same but the internal

critical stress is different and characteristic distribution of the internal critical stresses is present in a material. The second derivative of the hysteresis half-loop contains information on the effective stress and the probability density distribution of the critical internal stresses.

The aim of the present paper is to study the cyclic plasticity of this superalloy at temperatures 23, 500 and 800 °C, evaluate the cyclic stress-strain curves, analyze surface relief produced by cyclic straining and adopting the analysis of the hysteresis loop find and differentiate the sources of the cyclic strength.

## Experimental

Inconel 738LC polycrystals were provided by PSB Turbo, Velká Bíteš a.s. as conventionally cast rods in fully heat treated condition. Chemical composition of the superalloy is 16.22 Cr, 8.78 Co, 2.63 W, 1.71 Mo, 1.77 Ta, 3.37 Ti, 3.35 Al, 0.84 Nb, 0.2 Fe, 0.1 C, 0.04 Zr, 0.008 B, the rest Ni (all in wt. %). The structure of superalloy consisted of large  $\gamma$  grains with dendritic morphology,  $\gamma/\gamma'$  eutectic, carbides and shrinkage pores up to 0.16 mm in diameter (see Fig. 1a). The average grain size determined by the linear intercept method was 3 mm. After the heat treatment  $\gamma'$  precipitates are formed with near-cuboidal shape. They have an average diameter of 670 nm (see Fig. 1b). TEM study revealed the presence of 56 % volume fraction of the  $\gamma'$  precipitates.

The low cycle fatigue tests were performed on button-end specimens having the gauge length

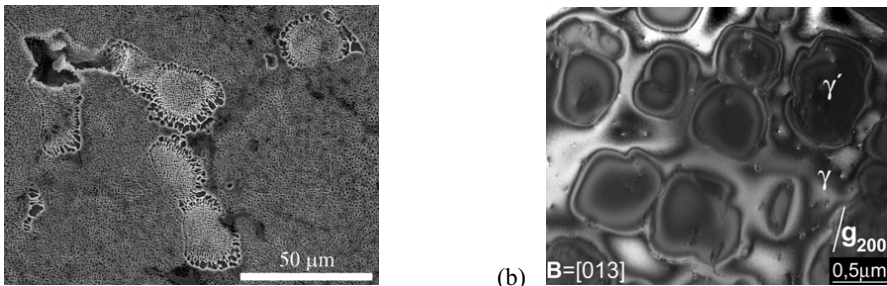


Fig. 1. Microstructure of IN 738LC (a) SEM, (b) TEM (in the dark field).

and the diameter of 15 and 6 mm, respectively. They were fatigued in a computer controlled electro-hydraulic MTS testing system at total strain rate of  $1 \times 10^{-3} \text{ s}^{-1}$  with fully reversed total strain cycle ( $R_\epsilon = -1$ ). Strain was measured and controlled using a sensitive extensometer with a 12 mm base. The tests were conducted at room temperature (23 °C), 500 and 800 °C in air. The strain history at each temperature was similar to that as applied during multiple step test on one specimen. The sampling rate was 1 ms, and thus even the smallest hysteresis loop contained more than 2000 stress-strain data. Using maximum and minimum strains in a cycle, the relative strain,  $\epsilon_r$ , and the relative stress,  $\sigma_r$ , were calculated for the tensile and for the compressive hysteresis half loops [6]. The first and the second derivatives of hysteresis half loops were obtained using smoothing numerical procedures. For each point of the first and of the second derivatives the number of the neighbour points involved in their determination could be chosen. The hysteresis loops for selected numbers of cycles were saved to disk memory. Plastic strain amplitude were derived from the half of the loop width.

Internal structure was observed in TEM Philips CM-12 using the technique of oriented foils. For surface relief observations all specimens fatigued were mechanically and electrolytically polished before cycling. They were observed in SEM JEOL JSM6460.

## Results

Figure 2 shows the dependence of the stress amplitude  $\sigma_a$  on the number of cycles  $N$  obtained at all temperatures during the test at increasing levels of total strain amplitude at constant strain rate equal to  $1 \times 10^{-3} \text{ s}^{-1}$ . The stabilized stress response is observed for low amplitudes at all temperatures. At room temperature the cyclic hardening is observed in cycling with amplitudes above  $4 \times 10^{-3}$  (see Fig. 2). At temperature  $500 \text{ }^\circ\text{C}$  cyclic hardening is apparent at all strain amplitudes with the exception of the lowest strain amplitude. The hardening becomes more pronounced with increasing strain amplitude. At temperature  $800 \text{ }^\circ\text{C}$ , the initial cyclic hardening is followed by the very mild and slow softening, which is typical for high amplitudes. Approximately stabilized behaviour was observed.

Table 1. Parameters of cyclic stress-strain curves.

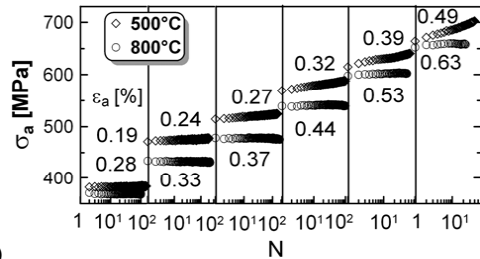
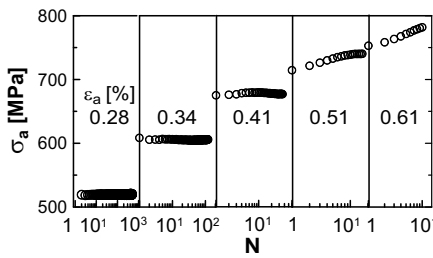


Fig. 2. The cyclic hardening/softening curves of IN 738LC at (a)  $23 \text{ }^\circ\text{C}$  and (b)  $500$  and  $800 \text{ }^\circ\text{C}$ .

Temperature	[ $^\circ\text{C}$ ]	23	500	800
$K'$	[MPa]	1 970	1 950	1 840
$n'$	[-]	0.137	0.147	0.158
$E$	[GPa]	180	187	130

Table 2 Effective stresses of two phases at three temperatures.

Temperature	[ $^\circ\text{C}$ ]	23	500	800
$\sigma_{eff}(\gamma)$	[MPa]	$\sim 100$	$\sim 90$	170
$\sigma_{eff}(\gamma')$	[MPa]	$\sim 550$	$\sim 550$	540

Cyclic stress-strain curves (CSSCs) were derived from the last hysteresis loop within each loading block and represent the cyclic stress-strain curves obtained using a short-cut procedure. They are plotted in Fig. 3 for all three temperatures as a function of the stress amplitude vs. plastic strain amplitude. Experimental data were approximated by the power law in the form  $\sigma_a = K' (\epsilon_{ap})^{n'}$ . Parameters of this dependence, i.e. the fatigue hardening coefficient  $K'$  and the fatigue hardening exponent  $n'$ , were evaluated using linear regression analysis and are shown in Table 1. The position of the CSSC depends on the temperature and with increasing temperature the stress amplitude decreases and the fatigue hardening exponent increases.

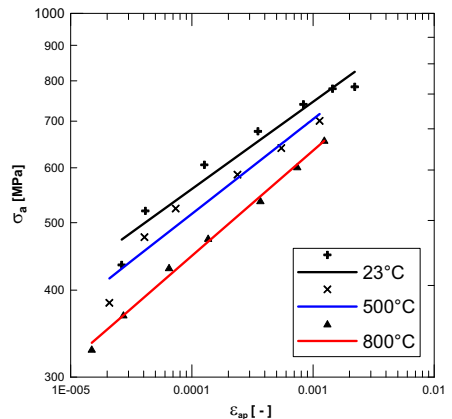


Fig. 3. The CSSCs of In738LC at three temperatures.

Saturated hysteresis loops obtained from the last step of the multiple step test were recorded at all three temperatures of cycling. They are shown in Fig. 4 and correspond to approximately the same amplitude of plastic strain  $\sim 1.4 \times 10^{-3}$ . The shape of the half-loops was analyzed by plotting the first and the second derivatives of tensile half-loops (divided by effective modulus  $E_{eff}$  or by the half of the square of effective modulus) vs. relative strain  $\epsilon_r$  or vs. fictive stress  $\epsilon_r E_{eff} / 2$  (Figs 5 to 7) [6].

The effective modulus  $E_{eff}$  is found from the first derivative at relative strain where the second derivative reaches its first minimum. The initial drop of the second derivative until the first minimum corresponds to the relaxation of the plastic strain under decreasing effective stress. The plots of the first and the second derivatives of a two-phase alloy with phases having different critical internal stresses and their evolution with the number of cycles are displayed for all three temperatures in Figs 5 to 7. Two peaks of the second derivative that approximate the probability density function (PDF) of the critical internal stresses are present. They correspond to the subsequent plastic deformation of  $\gamma$  and  $\gamma'$  phases within a cycle. The second peak is well developed

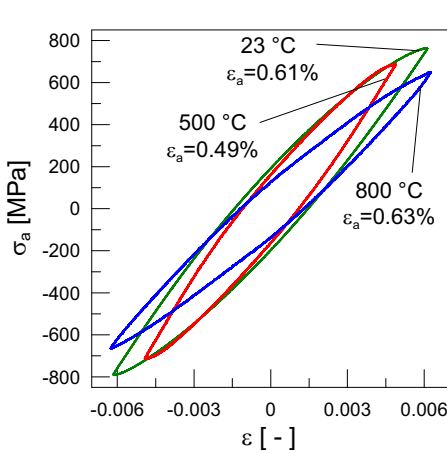
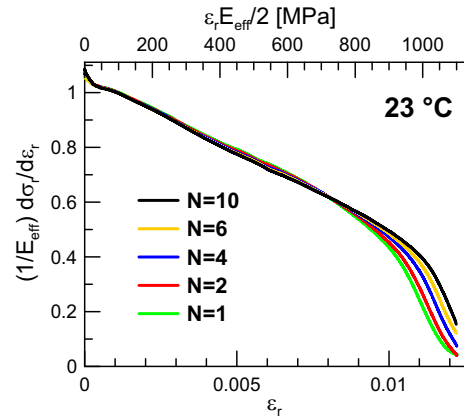
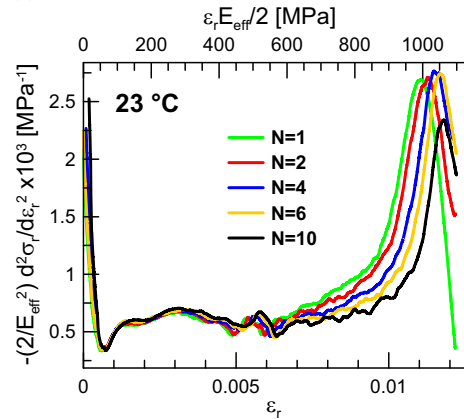


Fig. 4. The saturated hysteresis loops at 23 °C cycled with  $\epsilon_a = 0.61\%$ , at 500 °C, with  $\epsilon_a = 0.49\%$  and at 800 °C with  $\epsilon_a = 0.63\%$ .

for all three temperatures and changes with increasing number of loading cycles. Both peaks are most pronounced at elevated temperatures. The position of the second peak changes appreciably only in cyclic straining at 23 °C and at 500 °C. His position is moving to higher fictive stresses, which corresponds to the cyclic hardening. It is in agreement with observed hardening (see Fig. 2) The effective stresses of both phases were estimated from the relative strain where starts the corresponding peak of PDF. The analysis of the hysteresis loop shape in room temperature cyclic straining (Fig. 5) reveals only poorly defined first maximum. The second maximum is well developed and is shifted to higher fictive stresses

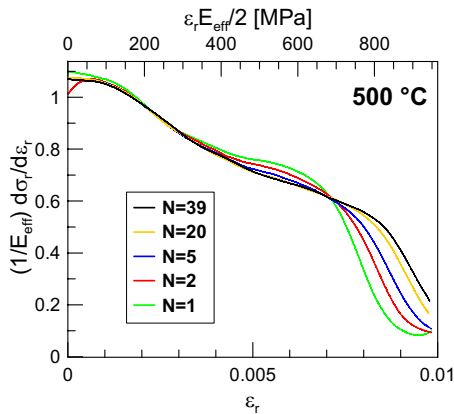


(a)

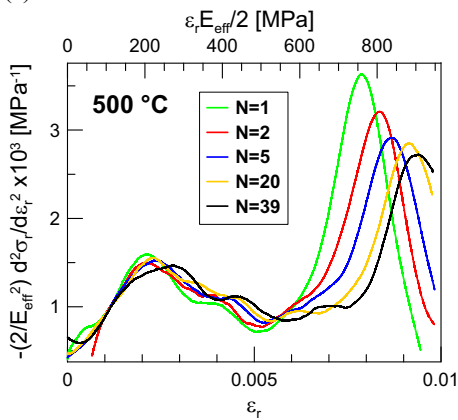


(b)

Fig. 5. The first and the second derivatives of the tensile half-loops (from Fig. 4) in relative coordinates in cycling at 23 °C.  $E_{eff} = 180$  GPa.

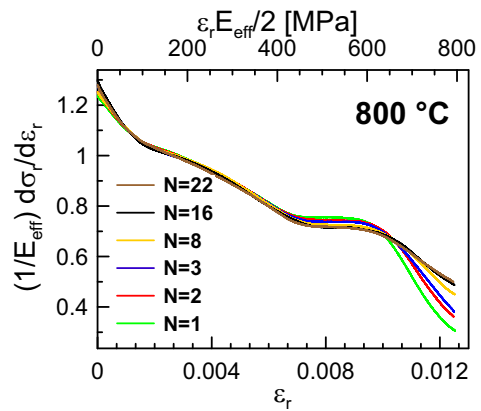


(a)

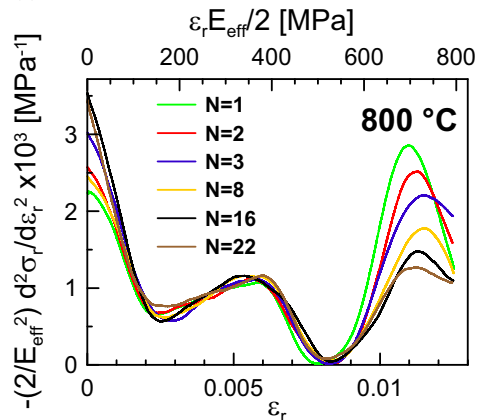


(b)

Fig. 6. The first and the second derivatives of the tensile half-loops (from Fig. 4) in relative coordinates in cycling at 500 °C,  $E_{eff} = 193$  GPa.



(a)



(b)

Fig. 7. The first and the second derivatives of the tensile half-loops (from Fig. 4) in relative coordinates in cycling at 800 °C.  $E_{eff} = 127$  GPa.

during cyclic straining. At 500 and 800 °C (Figs 6 and 7) two well separated peaks on the plot of the second derivative are observed. The effective stresses of  $\gamma$  and  $\gamma'$  phases at different temperatures can be estimated only approximately and the estimated values are displayed in Table 2. Unambiguous value of the effective stress in  $\gamma$  and  $\gamma'$  phases was found only in cycling at 800 °C. The effective stress in  $\gamma'$  phase is high and is in agreement with the difficult movement of dislocations in an ordered structure.

Surface topography of selected specimens cycled to fracture at three temperatures has been studied using the scanning electron microscope. Figures 8 to 10 show the characteristic surface relief of specimens cycled with the strain amplitudes shown in Fig. 4 that correspond to the saturated plastic strain amplitude  $\sim 1.4 \times 10^{-3}$  at a particular temperature. Parallel slip markings were identified in specimens cycled at all three temperatures. At room temperature (Fig. 8a) they often seem to run along the whole grain, however, microscopically, the markings are interrupted and a parallel marking continues in the previous direction. Slip markings were identified as extrusions having varying height. They cut both the matrix and  $\gamma'$  precipitates. At 500 °C (Fig. 9) finer

markings with high density covering the whole grain were observed. Random distribution of slip markings with pronounced geometry consisting from a high extrusion and parallel intrusion are found at 800°C. The presence of distinct slip markings found at all three temperature during cyclic loading indicates cyclic slip localization.

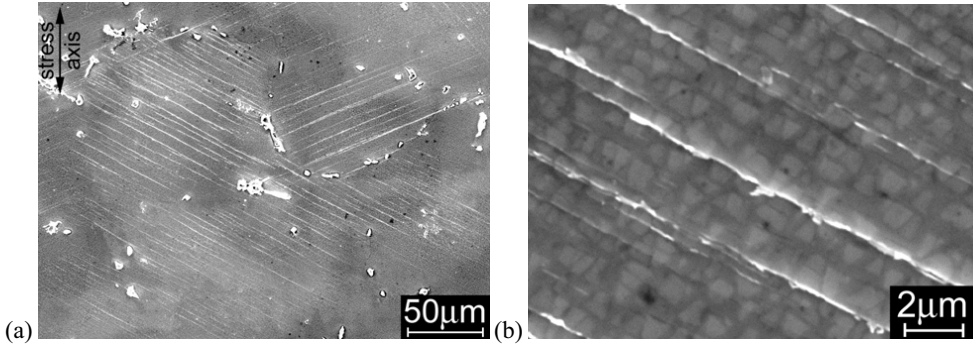


Fig. 8. SEM micrograph of surface relief in cyclic straining at 23 °C of IN 738LC (a) overall view (b) detail

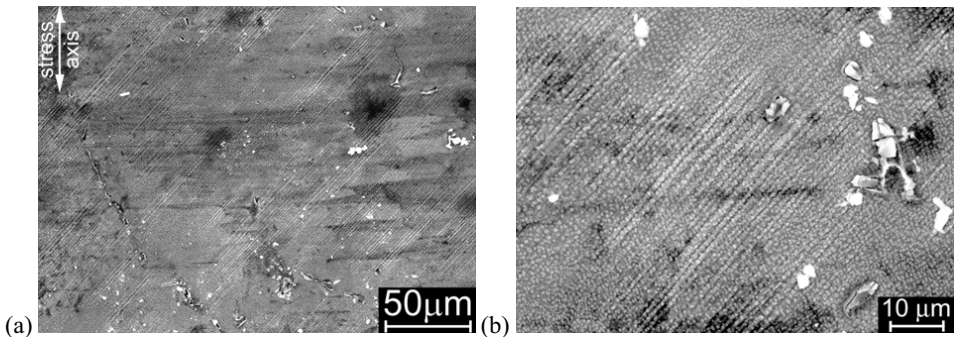


Fig. 9. SEM micrograph of surface relief in cyclic straining at 500 °C of IN 738LC (a) overall view (b) detail.

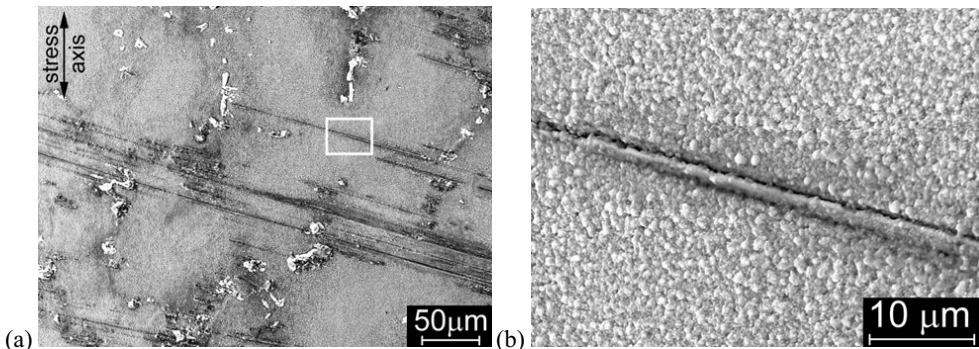


Fig. 10. SEM micrograph of surface relief in cyclic straining at 800 °C of IN 738LC (a) overall view (b) detail.

## Discussion

The study of the cyclic stress-strain response of IN 738LC superalloy and the observation of the surface slip markings in specimens cycled at room and at elevated temperatures yield important information on the type of the cyclic straining and the sources of the cyclic stress at different temperatures. The drop in the stress response when the temperature is increased to 800 °C, as documented by cyclic stress-strain curves, is only around 100 MPa. It witnesses a good resistance of this alloy to high temperature cyclic loading. The observation of the surface relief proves that cyclic plastic strain is highly localized into persistent slip bands, which are thin and pass through both the  $\gamma$  matrix and  $\gamma'$  precipitates. As a result slip markings, or persistent slip markings are produced on the surface of individual grains. They consist preferentially of parallel extrusions with density depending on the temperature of cycling. At the highest temperature the width and the height of the extrusions was the larger than at lower temperatures and the extrusion was accompanied by a parallel intrusion. Presumably, extrusions are present at all temperatures, however, standard SEM techniques cannot identify them [9].

Due to localization of the cyclic plastic strain the stress-strain response of IN 738LC superalloy reflects the cyclic straining only in localized volume with local plastic strain more than an order of magnitude higher than the applied plastic strain amplitude. Nevertheless, macroscopic stress-strain response reflects both the local stress-strain behaviour and the degree of cyclic strain localization.

Measurement of the hysteresis loop at different temperatures and its subsequent analysis using statistical theory of the hysteresis loop allows obtaining a more detailed view of the sources of the cyclic stress. Two peaks reproducibly identified on the second derivative of the hysteresis half-loop represent the distribution of the internal critical stresses in this cyclically strained two-phase structure. From the positions of minima of the second derivative of the hysteresis half-loop the effective stresses of  $\gamma$  and  $\gamma'$  phases were estimated at three temperatures. The effective stress of the  $\gamma$  phase is low but has increased when the cycling temperature increased to 800 °C. This can be the result of continuous annihilation of dislocations in soft  $\gamma$  phase at elevated temperature and resulting drop of dislocation density compensated by high dislocation velocities and thus the increased effective stress.

The effective stress of the  $\gamma'$  phase could be precisely found only at temperature 800 °C but approximate estimate at other two temperatures shows that this quantity is nearly temperature independent. The higher stress response of the material at 500 °C and 23 °C in comparison with that at 800 °C is due to systematic shift of the peak corresponding to  $\gamma'$  phase to higher stresses with increasing number of cycles resulting in cyclic hardening. Contrary to cyclic straining at lower temperatures the position of the second peak in the second derivative at 800 °C is nearly constant (see Fig. 7).

Previous TEM study of the internal dislocation structure in a related IN 713LC alloy [10] revealed localized cyclic plastic straining in the planar bands parallel to  $\{111\}$  planes up to temperature 800 °C. The stress components thus correspond to the dislocation arrangement and dislocation velocities in the bands of intensive glide. The cyclic hardening observed at temperatures below 500 °C is connected with the continuous increase of the dislocation density in the channels and resulting shift of the second peak of the probability density distribution of the internal critical stresses. In high temperature straining the continuous recovery of the  $\gamma$  phase leads to stabilized stress response.

## Conclusions

The results of total strain controlled fatigue tests in symmetrical strain cycling and the observations of surface relief produced by cyclic straining in cast Inconel 738LC polycrystals at 23, 500 and 800 °C can be summarized as follows:

1. Cyclic straining at temperatures up to 500 °C results in cyclic hardening, while at 800°C nearly stabilized behaviour is observed.
2. Cyclic stress-strain curves of Inconel 738LC obtained using short-cut procedure exhibit only weak temperature dependence up to 800 °C.
3. The analysis of the hysteresis loop based on statistical theory of the hysteresis loop allows estimating the contributions of the effective stress and the distribution of the critical internal stresses.
4. Cyclic plastic strain is highly localized into persistent slip bands. The macroscopic cyclic stress-strain response reflects the localized stress-strain response and the degree of cyclic strain localization.
5. High stress response of the Inconel 738LC superalloy at high temperature is due to high effective stress in the  $\gamma'$  phase.

### Acknowledgements

This research was supported by the grants No. 106/08/1631 and 106/07/1507 of the Czech Science Foundation and No. AV0Z 20410507 and A100480704 of the Academy of Sciences of the Czech Republic.

### References

- [1] M.J. Donachie, S.J. Donachie: *Superalloys: A Technical Guide*. (ASM Internat. Materials Park, USA, 2002).
- [2] Z. Mazur, A. Luna-Ramírez, J.A. Juárez-Islas and A. Campos-Amezcuca: *Eng. Failure Analysis* Vol.12 (2005), p. 474.
- [3] G. Jianting and D. Ranucci: *Int. J. Fatigue* Vol. 5 (1983), p. 95.
- [4] G. Jianting, D. Ranucci and E. Picco: *Mater. Sci. Eng.* Vol. 58 (1983), p. 127.
- [5] R.P. Wahi, J. Auerswald, D. Mukherji, A. Dudka, H.-J. Fecht and W. Chen: *Int. J. Fatigue* Vol. 19 (1997), p. S89.
- [6] J. Polák: *Cyclic Plasticity and Low Cycle Fatigue Life of Metals*. (Elsevier, Amsterdam, 1991).
- [7] J. Polák, F. Fardoun and S. Degallaix: *Mater. Sci. Engng* Vol. A297 (2001), p. 144.
- [8] J. Polák, F. Fardoun and S. Degallaix: *Mater. Sci. Engng* Vol. A297 (2001), p. 154.
- [9] J. Polák, J. Man, K. Obrtlík K. and T. Kruml: *Z. Metallkd.* Vol. 94 (2003), p. 1327.
- [10] M. Petrevec, K. Obrtlík and J. Polák: *Mater. Sci. Engng.* Vol. A400-401 (2005), p. 485.